INFLUENCE OF DURATION ON SEISMIC PERFORMANCE OF LAYERED SLOPES USING HAZARD-CONSISTENT GROUND MOTIONS

Wenqi Du[(1)], Wei Wang[(2)]

[(1)] *Professor, State Key Laboratory of Water Resources and Hydropower Engineering Science, Wuhan University, Wuhan 430072, China, wqdu309@whu.edu.cn*
[(2)] *Ph.D. student, State Key Laboratory of Water Resources and Hydropower Engineering Science, Wuhan University, Wuhan 430072, China, wangwei@whu.edu.cn*

Abstract

Assessing the dynamic stability of slopes during earthquakes is an important topic in geotechnical earthquake engineering. Recently occurred giant earthquakes (e.g., 2011 Tohoku earthquake) producing many high-amplitude and long-duration ground motions, have caused numerous landslides and unstable slopes over a large regional scale. The important role of amplitude- and frequency-related ground motion parameters (e.g., peak amplitude) on dynamic response of slopes has been widely acknowledged, whereas the role of ground-motion duration influencing the slope dynamic performance is still a subject of debate. Therefore, it is important to understand the role of ground motion duration on trigging landslides in a quantitative way, by isolating its effect using hazard-consistent ground motions. In this study, the duration effect on dynamic response of a multi-layer slope is quantitatively investigated, using hazard-consistent ground motion suites selected based on the generalized intensity measure distribution approach. One earthquake scenario with moment magnitude 7, rupture distance 20 km, and rock site condition is considered. Under this scenario, two hazard-consistent ground motion suites with different distributions of duration (relatively shorter- and longer-duration cases, respectively), are selected from the NGA-West2 database. The significant duration parameter $Ds_{5\text{-}75}$, defined as the time interval over which 5-75% of Arias intensity is accumulated, is adopted as the ground motion duration metric. Stress-deformation numerical analyses are then conducted using the ground motion suites selected for a generic slope model implemented in *FLAC*. The effect of ground motion duration on the dynamic slope performance is investigated by extensive comparisons. The input seismic hazard level that may affect the degree of the duration effect is also scrutinized. It is found that a longer-duration record suite has a higher possibility to cause a reduction of ground motion amplification, and an enlarged permanent displacement for a slope system. Based on the results demonstrated, one can make a fair judgment about the duration effect, in order to achieve a more accurate assessment about seismic performance of slopes in engineering applications.

Keywords: significant duration; hazard-consistent ground motions; ground motion selection; seismic slope performance; stress-deformation analysis

1. Introduction

Seismic stability assessment of geotechnical slope systems (e.g., earth/rockfill dam, earth slope, and earth embankment) is one of the most important issues in geotechnical engineering practice. There are three commonly used methods to assess the seismic stability of slopes [1]: pseudostatic analysis, permanent displacement analysis, and stress-deformation numerical analysis (e.g., finite-element method). In recent years, with the aid of computer technology development, the advanced numerical analysis has been increasingly applied to a variety of site-specific slope-system projects, providing more accurate estimation of the dynamic response of slopes.

Duration is one of the most important characteristics of earthquake ground motions. A longer-duration ground motion record associated with more energy and numbers of cycles, is likely to bring in a greater response and potential damage to geotechnical structures. Many researchers (e.g., [2-5]) have studied the effect of ground-motion duration on the dynamic response of soil layers and geotechnical structures. Nowadays it is widely acknowledged that ground motion duration could greatly affect the liquefaction potential of saturated loose sands [6]. Besides, a recent study [7] concluded that long ground-motion duration can greatly exacerbate the nonlinear effect of the pile responses on saturated sands. Yet, the role of ground motion duration in the seismic performance of slope structures remains ambiguous. Based on the Newmark-type slope displacement procedure [8], many studies (e.g., [9-11]) have stated that the influence of duration on earthquake-induced slope displacement is negligible; on the other hand, based on the so-called decoupled approach, Bray and Rathje [12] reported a significant influence of duration of input motions on slope permanent displacement, proposing seismic design charts with normalized duration parameters. Therefore, more research efforts should be made on this topic.

To conduct numerical time-history analysis on slope models, a suite of ground motions is commonly required as input. The input motions should properly reflect the shaking characteristics at a hazard-specific level, usually represented by a target spectrum (e.g., design spectrum). Numerous methods are available in literature regarding how to select 'appropriate' ground motion records. Specifically, some studies [13-16] emphasized that ground motions well capturing the statistical distribution (i.e., both mean and variance) of a target spectrum should be selected. A few of ground motion selection approaches have thus been developed, such as the conditional spectrum-based method [14], generalized intensity measure distribution (GIMD) method [15], as well as the generalized conditional intensity measure (GCIM) method [16]. These methods could be used to select hazard-consistent (i.e., consistent statistical distribution of the target spectrum) ground motions for dynamic analysis.

The aim of this paper is thus to investigate the influence of duration on dynamic performance of layered slopes, using selected hazard-consistent ground motions. Under a given earthquake scenario, two ground motion suites, which have a similar distribution of the response spectra but divergent distributions of duration, are selected using the foregoing GIMD approach. A generic numerical slope model is implemented in software *FLAC* [17], by which stress-deformation analysis can be conducted based on a finite-difference algorithm. Using the two ground motion suites selected as inputs, the resulting slope dynamic performances is then compared in detail to scrutinize the duration effect on slope responses. Based on the comparative results obtained, some discussions and concluding remarks are finally provided.

2. Selecting Hazard-consistent Ground Motion Suites

2.1 GIMD-based ground motion selection approach

The procedure of the GIMD-based ground motion selection approach is briefly introduced as follows. First, a vector of intensity measures (IMs) can be assumed to follow a multivariate normal distribution in logarithmic space [18]. Second, under a given earthquake scenario (i.e., moment magnitude M_w, rupture distance R_{rup}, *etc*), the logarithmic mean $\mu_{\ln IM}$ and the standard deviation $\sigma_{\ln IM}$ can be obtained using a ground motion prediction equation (GMPE) for each IM. Thus, a suite of IM vectors can be simulated following the distribution as:

$$\ln IM^{simu} = \boldsymbol{N}\left(\boldsymbol{\mu}_{\ln IM}, \Sigma_{\ln IM}\right) \tag{1}$$

where $\boldsymbol{\mu}_{\ln IM}$ and $\Sigma_{\ln IM}$ denote the logarithmic means and covariance matrix of the vector-IM, respectively; $\boldsymbol{N}$ denotes multivariate normal distribution. Note that $\Sigma_{\ln IM}$ can be constructed by combining $\sigma_{\ln IM}$ and the emprical correlations between IMs (e.g., [18]).

Third, hundreds of realizations of the simulated IM vectors can be obtained based on Eq. (1); among these realizations, the set that best represents the assigned statistical distribution (i.e., $\boldsymbol{\mu}_{\ln IM}, \Sigma_{\ln IM}$) can be regarded as the optimal simulated set. Forth, for each simulated IM-vector in the optimal set, one (scaled or un-scaled) recorded ground motion can be selected to best match the simulated IM-vector. A weighted sum of squared errors (WSSE) can be used to quantify the mismatch between the simulated and the recorded one, expressed as:

$$WSSE = \sum_{i=1}^{N_{im}} \left[\ln IM_i^{simu} - \ln(SF^{\alpha} \cdot IM_i^{record})\right]^2 \tag{2}$$

where IM_i^{simu} is the i-th (i=1, 2, …N_{im}) IM value of the simulated optimal set; SF denotes the scale factor and α is used to differentiate the effect of SF on various IMs (e.g., α=1 for spectral acceleration SA); N_{im} is the number of IMs considered; and IM_i^{record} is the i-th IM value of a recorded ground motion.

Finally, by repeating the forth step for each simulated IM-vector, an ensemble of ground motion records can be selected, whose statistical distribution of this IM-vector appropriately follows the prescribed statistical distribution as is shown in Eq. (1). Note that some stastistical metrics, such as K-S test statistic, can also be used to further refine the selected ground motion suite. A detailed description about this ground motion selection algorithm can be found in Du and Wang [15].

2.2 Two ground motion suites selected for subsequent numerical analysis

Following the ground motion selection algorithm listed in Section 2.1, a suite of recorded ground motions can be selected with the IMs matching the target distribution of a vector-IM. Therefore, by considering different 'targets', two suites of ground motions can be selected, with a consistent distribution of SAs but divergent distributions of duration metric.

The first step of selecting ground motion records is to determine the target vector-IM. The significant duration parameter $Ds_{5\text{-}75}$, defined as the time interval over which 5%-75% of Arias intensity is accumulated, is considered as the ground motion duration metric. Therefore, the target vector-IM consists of $Ds_{5\text{-}75}$ and SA ordinates at 22 periods (ranging from 0.01 s to 10 s).

An earthquake scenario of M_w = 7 is assumed to occur on a strike-slip fault zone. A hypothetic 10-meter-high slop is located at a bedrock site (time-averaged shear wave velocity in upper 30 meters, V_{s30}=760 m/s), with the source-to-site distance assumed as 20 km. The Campbell and Bozorgnia GMPE [19] and the Du and Wang model [20] are used to compute the statistical distributions (i.e., medians and standard deviations) of SAs and $Ds_{5\text{-}75}$, respectively. The median peak ground acceleration (PGA) for this scenario is computed as 0.17 g. The Jayaram and Baker [18] and Bradley [21] empirical correlation models are adopted to help construct the covariance matrix (i.e., $\Sigma_{\ln IM}$ in Eq. (1)) for this vector-IM.

The specified target means for two cases are illustrated in Table 1. It is clear that both cases have the actual target means for SA, whereas the target means of $Ds_{5\text{-}75}$ are deliberately amplified and reduced for Cases 1 and 2, respectively. It is thus anticipated that the selected ground motions for both cases would exhibit a similar distribution of response spectra (therefore 'hazard-consistent'), while the $Ds_{5\text{-}75}$ distribution of Case 1 would be noticeably greater than that of case 2. Thus, the selected ground motions for the two cases can be used to explicitly examine the duration effect on seismic slope performance, which will be introduced in next session.

Table 1 - Various means of the target vector-IM for two cases considered

Ground motion group	SA(T)	$Ds_{5\text{-}75}$ $^{\xi}$
Case 1 (longer-duration set)	$\mu_{\ln SA}$	$\mu_{\ln Ds_{5-75}} + 0.5 \cdot \sigma_{\ln Ds_{5-75}}$
Case 2 (shorter-duration set)	$\mu_{\ln SA}$	$\mu_{\ln Ds_{5-75}} - 0.5 \cdot \sigma_{\ln Ds_{5-75}}$

$^{\xi}$: $\mu_{\ln Ds_{5-75}}$ and $\sigma_{\ln Ds_{5-75}}$ denote the predicted mean and standard deviation for $Ds_{5\text{-}75}$ based on the empirical model [20]

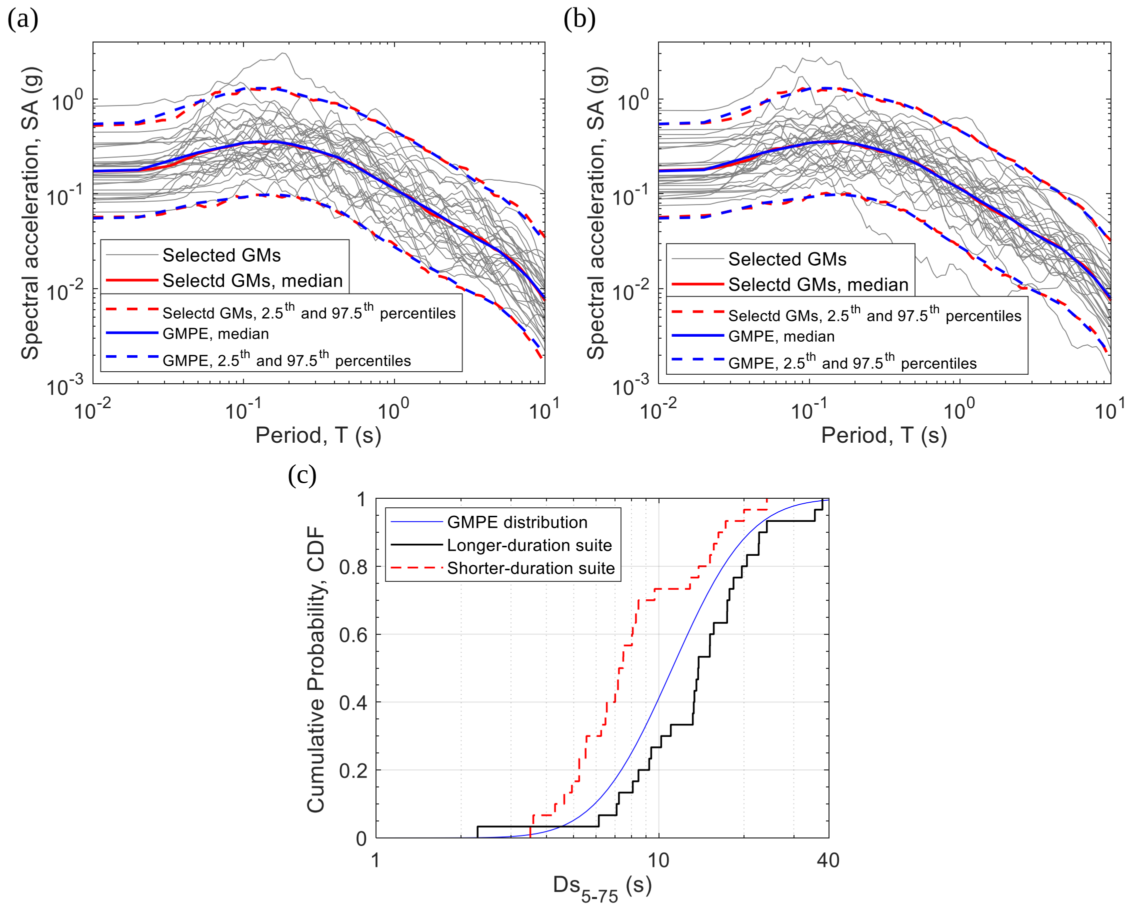

Fig. 1 – (a), (b): Spectral distributions of the selected ground motions for cases 1 and 2, respectively; (c) empirical CDFs of $Ds_{5\text{-}75}$ of the selected ground motion suites.

Fig. 1a and b display the response spectra of the selected ground motion suites for the longer-duration and shorter-duration suites, respectively. The median, 2.5th, and 97.5th percentiles of the selected spectra are also shown and compared to those of the GMPE-based target distribution. As shown from these two plots, the ground motion suites selected appropriately match the target (median and dispersion) distribution of SA ordinates. Besides, Fig. 1c shows the empirical cumulative distribution functions (CDFs) of $Ds_{5\text{-}75}$ for both suites, together with the actual distribution of $Ds_{5\text{-}75}$ computed using the empirical model. It is clearly that the ground motions selected for cases 1 and 2 exhibit an enlarged and a reduced distribution of $Ds_{5\text{-}75}$, respectively, being consistent with the assigned target means listed in Table 1.

Fig. 2 illustrates an example pair of the response spectra and (up-scaled) acceleration-time histories selected from case 1 and case 2, respectively. They are displayed herein due to a high degree of similarity regarding the spectral shape. Besides, as expected, the ground motion selected from case 1 has a notable longer duration than the one selected from case 2.

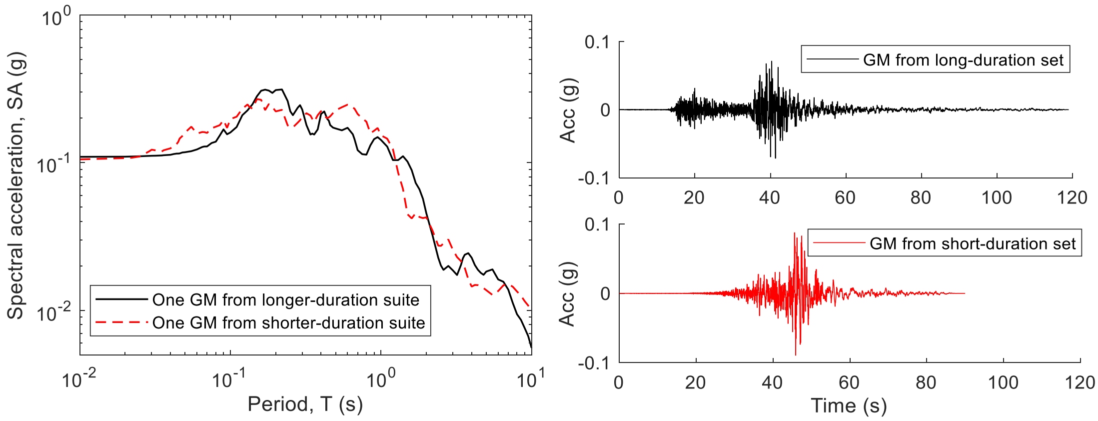

Fig. 2 – Plots of response spectra and ground motion acceleration-time histories for illustration of longer-duration and shorter-duration suite. GM: ground motion.

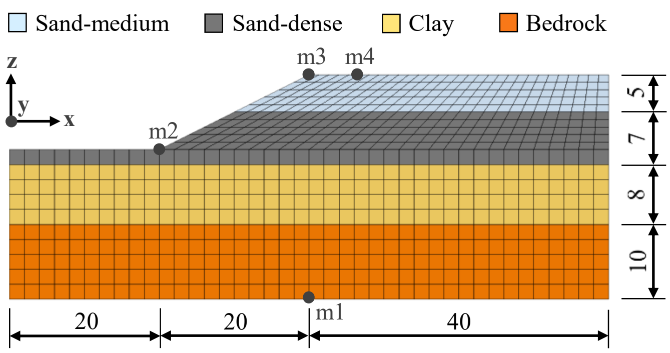

Fig. 3 – Schematic representation of a multi-layer slope (unit: m).

Table 2 – Type and physical parameters for each slope stratum

Stratum	Density ρ / kg · m^{-3}	Bulk modulus K_0 / MPa	Shear modulus G_0 / MPa	Reference strain γ_{ref} / %	Cohesion c / kPa	Friction φ / °
Sand-medium	2000	240	110	0.06	5	35.0
Sand-dense	2100	260	130	0.06	10	36.5
Clay	1800	750	150	0.20	75	20.0
Bedrock	2700	10200	7670	-	15000	45.0

3. Slope Model Development

3.1 Overview

To shed light on the influence of duration on seismic slope performance, a multi-layer slope model is implemented and illustrated in Fig. 3. The height and the inclination of the slope are assigned as 10 m and 26.5 °(i.e., 1:2), respectively. The strata of the model from top to bottom are sand-medium, sand-dense, clay, and bedrock, respectively; the soil parameters of each stratum are summarized in Table 2. Besides, to minimize the boundary effect, the distance between the slope crest to the right-side boundary is set as 4-

times of the slope height, and the distance of the slope toe to the left-side boundary is set as 2-times of the slope height. During the dynamic process, the acceleration-time histories and displacement-time histories at 4 points (i.e., m1-m4 as shown in Fig. 3) are monitored to evaluate the slope dynamic performance.

3.2 Constitutive model and soil modules degradation

The dynamic slope response subjected to a ground motion excitation is simulated using a modified constitutive model, which combines the hysteretic damping formulation with the well-known Mohr-Coulomb strength criterion. The modified constitutive model has been implemented in *FLAC* [17]. *FLAC* is numerical modeling software for geotechnical analysis, capturing the complex stress-deformation behavior of soil/geotechnical models by an explicit finite volume formulation. A modulus-reduction technique is applied to adjust the tangent shear modulus and damping ratio based on empirical model curves. In this study, the empirical shear modulus reduction function suggested by Hardin and Drnevich [22, 23] is used in the elastic stage:

$$M = \frac{1}{1+\gamma/\gamma_{\mathrm{ref}}}, \ \gamma \le \gamma_{\mathrm{m}} \tag{3}$$

where $M = G/G_0$ denotes the normalized shear modulus; γ is the shear strain; γ_{m} denotes the yield shear strain, which is determined by Mohr-Coulomb strength criterion; γ_{ref} is the reference strain corresponding to the strain at which the modulus reduction curve crosses the $M = 0.5$ line. When $\gamma > \gamma_m$, the soil stress-strain relationship is assumed to switch into the plastic stage. The modulus-reduction function could be expressed as follows based on the ideal plasticity hypothesis:

$$\frac{G}{G_{\mathrm{m}}} = \frac{\gamma_{\mathrm{m}}}{\gamma}, \ \ \gamma > \gamma_{\mathrm{m}} \tag{4}$$

where G_{m} denotes the yield secant shear modulus corresponding to γ_{m}.

Thus, the following formation can be obtained by substituting Eq. (3) into Eq. (4), expressed as:

$$M = \frac{1}{\left(1+\frac{\gamma_{\mathrm{m}}}{\gamma_{\mathrm{ref}}}\right)\frac{\gamma}{\gamma_{\mathrm{m}}}}, \ \gamma > \gamma_{\mathrm{m}} \tag{5}$$

For a stress-strain cycle consisting of initial loading and an unloading/reloading excursion, the expression of damping ratio D_r could be derived based on energy dissipation analysis [24]:

$$D_r = \frac{2\gamma_{\mathrm{ref}}}{\pi\gamma_{\mathrm{c}}}\left\{\frac{2\left(1+\gamma_{\mathrm{m}}/\gamma_{\mathrm{ref}}\right)}{\left(\gamma_{\mathrm{m}}/\gamma_{\mathrm{ref}}\right)^2}\left[\frac{\gamma_{\mathrm{m}}}{\gamma_{\mathrm{ref}}} - \ln\left(1+\gamma_{\mathrm{m}}/\gamma_{\mathrm{ref}}\right)\right] - 1\right\} + \frac{2\left(\gamma_{\mathrm{c}}-\gamma_{\mathrm{m}}\right)}{\pi\gamma_{\mathrm{c}}} \tag{6}$$

where γ_{c} denotes the cyclic shear strain, and the other parameters are defined as above.

Fig. 4 illustrates the normalized shear modulus reduction and damping ratio curves of sand and clay, respectively. In order to obtain a compatible starting state for both stress and strain, the hysteretic damping is needed at the static analysis stage to build up the initial stresses. Besides the hysteretic damping, viscous damping is also needed to exhibit some damping at small strains. A 0.2% stiffness-proportional component of Rayleigh damping is thus applied.

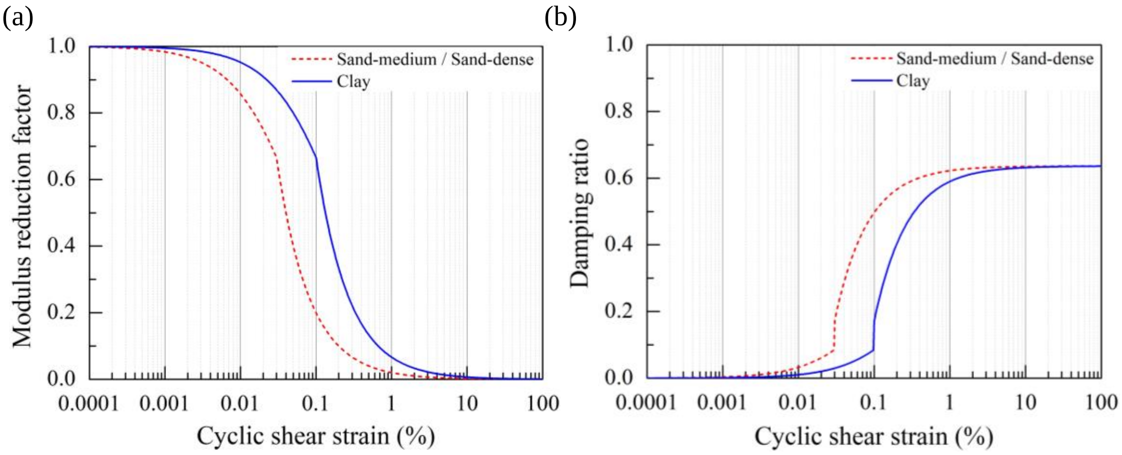

Fig. 4 – Normalized shear modulus curve and damping ratio curve of sand and clay used in this study.

3.3 Mesh size and boundary conditions

The mesh dimension should be carefully checked before performing a dynamic analysis, to avoid numerical distortion when propagating seismic waves. It is suggested in *FLAC* that the maximum mesh size should be smaller than approximately 1/10 to 1/8 of the wavelength corresponding to the highest frequency component of the input waves. The mesh size therefore varies from 1.3 m to 2.0 m according to the criterion described above. In the stage of the initial stress generation, the horizontal movement of both left and right sides is fixed, while the bottom boundary surface is completely fixed. In the stage of dynamic analysis, a free-field boundary is assigned to both lateral sides, and the horizontal movement (x-component) of the bottom boundary is allowed to apply the seismic excitations.

4. Dynamic Results of Numerical Analysis

4.1 Comparative results using the selected ground motion suites

Based on the generic slope model implemented in *FLAC*, dynamic analyses are performed using the two selected ground motion suites as input. For each time-history analysis, the acceleration- and displacement-time histories at the monitor points are tracked and recorded to reveal the slope dynamic performance. Two specific issues, namely the ground-motion amplification and the maximum permanent displacement, are discussed in this section.

Fig. 5a, b show the resultant response spectra corresponding to the response at slope crest (point m3) when subjected to the selected shorter-duration and longer-duration suites, respectively. It can be seen that the dispersions of the response spectra are generally similar. To better quantify the slope amplification effect, amplification factors are computed as the ratios of SAs at crest to the SAs at bedrock (i.e., $SA_{crest}/SA_{bedrock}$). For each ground motion suite, the mean amplification factors of the 30 ground motions are calculated. Comparative information about the mean amplification factors with respect to vibration period is provided in Fig. 5c, which clearly shows that the amplification effect obtained by the shorter-duration suite is slightly higher than that of the longer-duration one. Thus, using a ground motion suite with longer duration would perhaps yield a smaller amplification in terms of shaking intensities. In addition, for both cases, the amplification amplitudes are in the range of 1.5 to 4, whereas the peak amplification mostly occurs within the short period range (T<0.3 s).

Fig. 6 compares the cumulative results in terms of the maximum permanent displacement of this slope subjected to the two ground motions suites. It can be seen that although the distributions are generally similar, the maximum displacements calculated using the longer-duration suite are notably larger than the shorter-duration suite. The ratio of the median displacement of the longer-duration case to the shorter-duration one is appropriately 1.15. Recalling that as illustrated in Fig. 1, the two ground motion suites have consistent statistical distributions of SAs yet completely different distributions of $Ds_{5\text{-}75}$, therefore, it is confirmed that the ground motion duration plays a positive role in the dynamic performance of slopes (in terms of the sliding displacement).

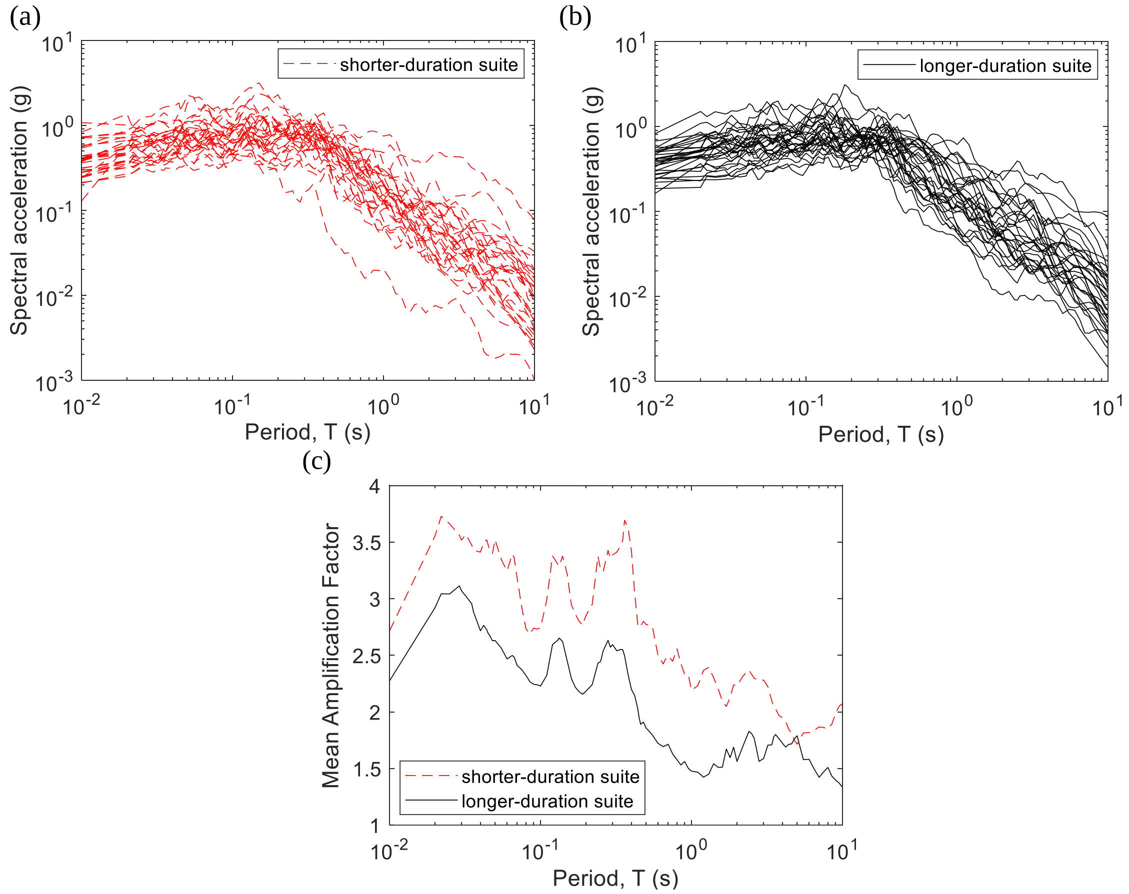

Fig. 5 – Response spectra at the crest of slope using the (a) shorter-duration and (b) longer-duration suite, respectively; (c) comparison of the mean amplification factors for the two selected ground motion suites.

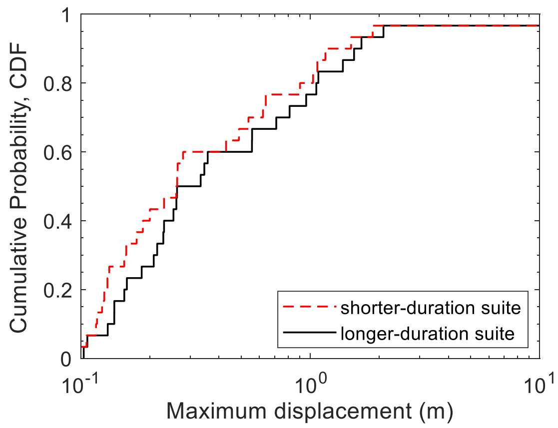

Fig. 6 – Cumulative distribution functions (CDFs) of the calculated maximum permanent displacements using the longer- and shorter-duration ground motion suites.

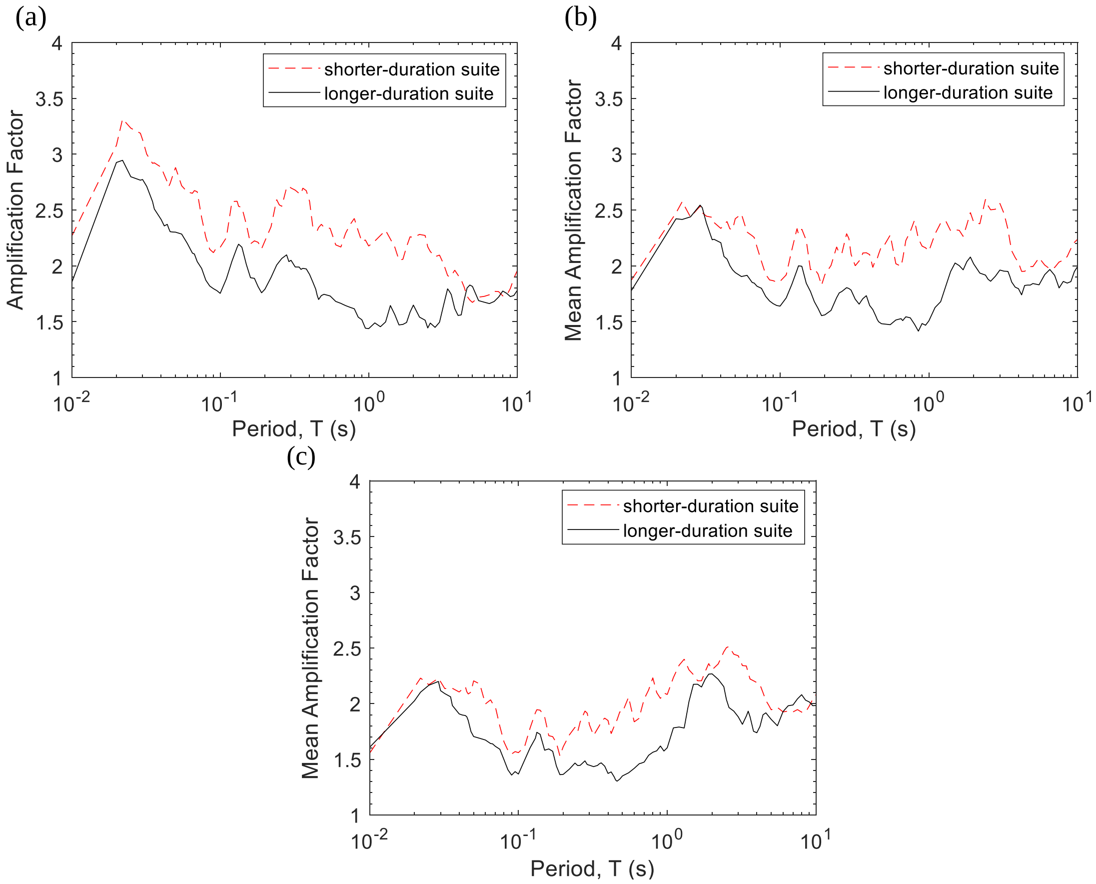

Fig. 7 – Mean amplification factors versus vibration periods when using up-scaled ground motion suites with scale factors of (a) 1.5, (b) 2.0, and (c) 2.5, respectively.

4.2 Role of the input hazard level

The preceding subsection describes a brief summary about the slope dynamic performance using the two ground motion suites selected. It is then tempting to further investigate the role of the earthquake hazard level in the duration effect on slope dynamic performance. In this subsection, both ground motion suites are up-scaled to a higher hazard level, with scale factors of 1.5, 2.0, and 2.5, respectively; the up-scaled target median PGA values are thus 0.26 g, 0.34 g, and 0.43 g, respectively. Dynamic analyses are then conducted for this generic slope using the up-scaled ground motion suites. Similarly, the amplification factors ($SA_{crest}/SA_{bedrock}$) at point m3 are computed for each suite. Fig. 7a, b, c display the resulting mean amplification factors for the up-scaled ground motion suites with scale factors of 1.5, 2.0, and 2.5, respectively. Two observations can be made. First, consistent with the observation in Fig. 5c, the amplifications resulting from the shorter-duration suite are generally higher than those of the longer-duration one. Second, as the earthquake hazard level increases, the amplification effect decreases, and the difference of the amplifications between two ground motion suites becomes less significant. Therefore, it appears that the duration effect on the reduction of slope amplifications will be smaller, if the input earthquake hazard is higher.

Fig. 8 illustrates the cumulative maximum displacements when using the three groups of up-scaled ground motions suites, respectively. As shown in Fig. 8a, b, the longer-duration ground motion suite yields a notably larger slope displacements compared to the shorter-duration one. This observation is consistent with Fig. 6. Yet, when a scale factor of 2.5 is used (Fig. 8c), the cumulative distributions of displacements for two cases (i.e., longer- versus shorter-duration suites) are generally similar. The ratios of the median displacements of the longer-duration suite to the shorter-duration one are 1.62, 1.35, and 1.06, corresponding to scale factors of 1.5, 2.0, and 2.5, respectively. Therefore, it is evident that using a longer-duration record suite possibly leads to an increase in the permanent sliding displacement of slopes; such increase in the displacement is more notable when the input hazard level is low-to-moderate (compared to the high seismic hazard case).

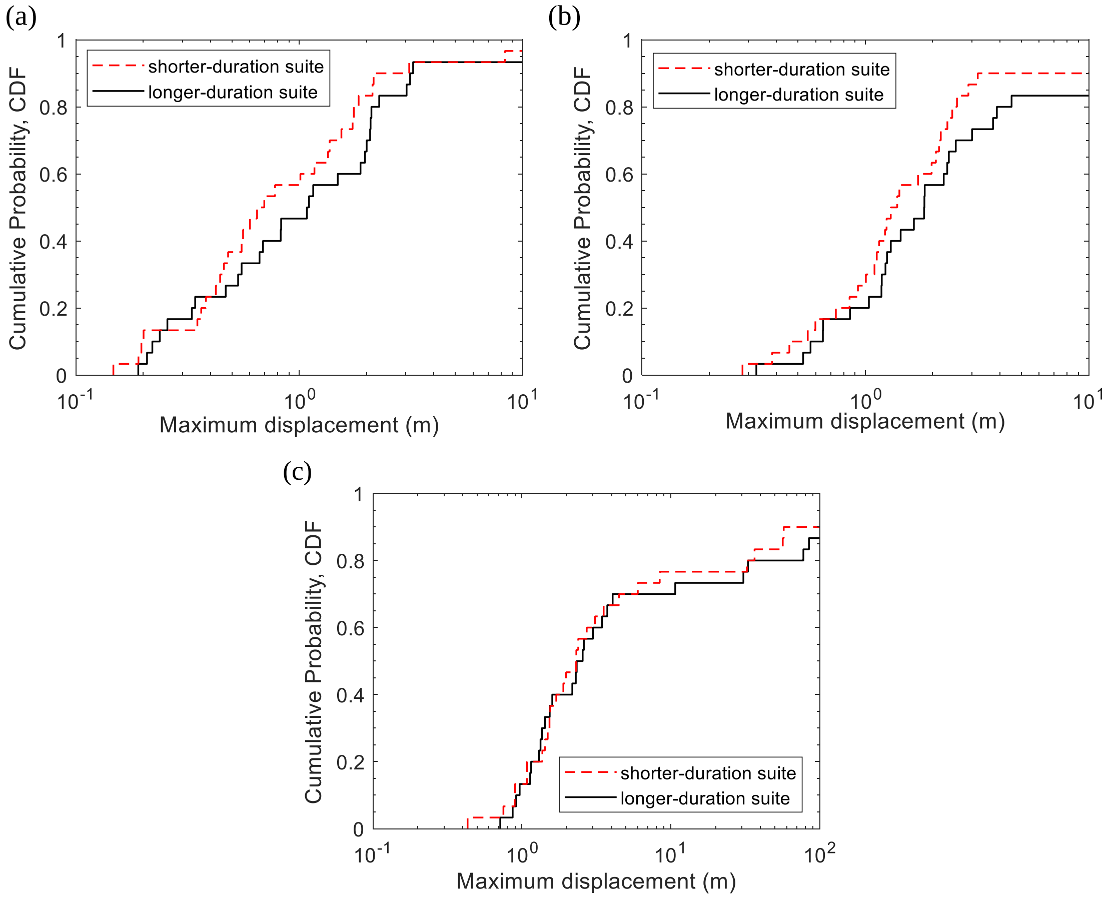

Fig. 8 –CDFs of the calculated maximum sliding displacements using the up-scaled ground motion suites with scale factors of (a) 1.5, (b) 2.0, and (c) 2.5, respectively.

5. Discussions and Conclusions

This paper studied the influence of ground-motion duration on the dynamic performance of slopes, using two selected hazard-consistent ground motion suites. A multi-layer generic slope was modelled in *FLAC*. Ground motion suites were selected based on the GIMD approach [15], using a target vector-IM comprising of response spectrum and significant duration parameter $Ds_{5\text{-}75}$. Under a M_w = 7 earthquake scenario, two ground motion suites were selected, exhibiting a consistent distribution of response spectra yet completely different distributions of $Ds_{5\text{-}75}$. A series of dynamic analyses were then conducted in *FLAC* using the ground motion suites selected; the acceleration- and displacement-time histories at slope crest were tracked during each analysis.

Comparative results of the analysis indicate that using the longer-duration ground motion suite leads to a slight reduction of ground-motion amplification and an increase of the slope permanent displacement. Therefore, when subjected to the longer-duration suite, the dynamic response (shaking intensity) of the slope is less severe, yet the slope performance (maximum permanent displacement) is much greater (compared to that of the shorter-duration one). This observation, however, contradicts with some studies stating that the duration influence on the slope sliding displacement is negligible. This discrepancy is mainly caused by the different methods employed. Specifically, those studies employed a simple Newmark-type stick-slip model which ignores the soil strength reduction during shaking process, whereas this study employs a complex numerical stress-deformation analysis.

An additional analysis was then conducted to examine the role of earthquake hazard level in the ground motion duration effect. As the input hazard level increases, the significance of the duration effect on both seismic wave amplification and slope displacement decreases. Thus, when the earthquake hazard is low-to-moderate, using a longer-duration record suite will possibly yield a reduction of slope amplification and an increase of the slope displacement; on the other hazard, when the seismic hazard is high (i.e., PGA>0.4 g), the duration effect on the dynamic slope performance is generally insignificant.

6. Acknowledgements

The authors acknowledge support from National Science Foundation of China (no. 51909193).

7. References

[1] Jibson RW (2011): Methods for assessing the stability of slopes during earthquakes—a retrospective. *Engineering Geology*, **122** (1), 43-50.

[2] Idriss IM, Boulanger RW (2006): Semi-empirical procedures for evaluating liquefaction potential during earthquakes. *Soil Dynamics and Earthquake Engineering*, **26** (2), 115-130.

[3] Green RA, Terri GA (2005): Number of equivalent cycles concept for liquefaction evaluations-revisited. *Journal of Geotechnical and Geoenvironmental Engineering*, **131** (4), 477-488.

[4] Seed HB, Lee KL (1966): Liquefaction of saturated sands during cyclic loading. *Journal of the Soil Mechanics and Foundations Division*, **92** (6), 105-134.

[5] Du W, Yu X, Ning CL (2020): Influence of earthquake duration on structural collapse assessment using hazard-consistent ground motions for shallow crustal earthquakes. *Bulletin of Earthquake Engineering*, accepted, in press.

[6] Kramer SL (1996): Geotechnical Earthquake Engineering. Practice Hall, New Jersey, pp. 653.

[7] Tombari A, El Naggar MH, Dezi F (2017): Impact of ground motion duration and soil non-linearity on the seismic performance of single piles. *Soil Dynamics and Earthquake Engineering*, **100**, 72-87.

[8] Newmark NM (1965): Effects of earthquakes on dams and embankments. *Géotechnique*, **15** (2), 139-160.

[9] Bray JD, Travasarou T (2007): Simplified procedure for estimating earthquake-induced deviatoric slope displacements. *Journal of Geotechnical and Geoenvironmental Engineering*, **133**, 381-392.

[10] Saygili G, Rathje EM (2008): Empirical predictive models for earthquake-induced sliding displacements of slopes. *Journal of Geotechnical and Geoenvironmental Engineering*, **134** (6), 790-803.

[11] Du W, Wang G, Huang D (2018): Evaluation of seismic slope displacements based on fully coupled sling mass analysis and NGA-West2 database. *Journal of Geotechnical and Geoenvironmental Engineering* ASCE, **144** (8): 6018006.

[12] Bray JD, Rathje ER (1998): Earthquake-induced displacements of solid-waste landfills. *Journal of Geotechnical and Geoenvironmental Engineering* ASCE, **124** (3): 242-253.

[13] Bradley BA (2010): A generalized conditional intensity measure approach and holistic ground-motion selection. *Earthquake Engineering and Structural Dynamics*, **39** (12): 1321-1342.

[14] Jayaram N, Lin T, Baker JW (2011): A computationally efficient ground-motion selection algorithm for matching a target response spectrum mean and variance. *Earthquake Spectra*, **27** (3): 797-815.

[15] Du W, Wang G (2018): Ground motion selection for seismic slope displacement analysis using a generalized intensity measure distribution method. *Earthquake Engineering and Structural Dynamics*, **47** (5): 1352-1359.

[16] Tarbali K, Bradley BA (2015): Ground motion selection for scenario ruptures using the generalised conditional intensity measure (GCIM) method. *Earthquake Engineering and Structural Dynamics*, **44** (10): 1601-1621.

[17] Itasca Consulting Group Inc (2005): FLAC-Fast Lagrangian Analysis of Continua. Version 5.0, User's Manual.

[18] Baker JW, Jayaram N (2008): Correlation of spectral acceleration values from NGA ground motion models. *Earthquake Spectra*, **24** (1): 299-317.

[19] Campbell KW, Bozorgnia Y (2014): NGA-West2 ground motion model for the average horizontal components of PGA, PGV, and 5% damped linear acceleration response spectra. *Earthquake Spectra*, 30(3): 1087-1115.

[20] Du W, Wang G (2017): Prediction equations for ground-motion significant durations using the NGA-West2 database. *Bulletin of the Seismological Society of America*, **107** (1): 319-333.

[21] Bradley BA (2011): Correlation of significant duration with amplitude and cumulative intensity measures and its use in ground motion selection. *Journal of Earthquake Engineering*, **15** (6): 809-832.

[22] Hardin BO, Drnevich VP (1972): Shear modulus and damping in soils: measurement and parameter effects. *Journal of the Soil Mechanics and Foundations Division ASCE*, **98** (SM6): 603-624.

[23] Hardin BO, Drnevich VP (1972): Shear modulus and damping in soils: design equations and curves. *Journal of the Soil Mechanics and Foundations Division ASCE*, **98** (SM7): 667-692.

[24] Kolsky, H (1963): Stress waves in solids. New York: Dover Publications.

